Lens Distortion Correction and Enhancement Based on Local Self-similarity for High-quality Consumer Imaging Systems

Article *in* IEEE Transactions on Consumer Electronics · February 2014

DOI: 10.1109/TCE.2014.6780920

CITATIONS
10

READS
622

5 authors, including:

Jinho Park
Chung-Ang University
20 PUBLICATIONS **48** CITATIONS
SEE PROFILE

Junghoon Jung
Samsung
30 PUBLICATIONS **133** CITATIONS
SEE PROFILE

Joonki Paik
Chung-Ang University
503 PUBLICATIONS **4,722** CITATIONS
SEE PROFILE

Lens Distortion Correction and Enhancement Based on Local Self-similarity for High-quality Consumer Imaging Systems

Donggyun Kim, *Student Member*, IEEE, Jinho Park, *Student Member*, IEEE, Junghoon Jung, Taechan Kim, *Senior Member*, IEEE and Joonki Paik, *Senior Member*, IEEE

Abstract — *In this paper, a novel image enhancement system for a wide-angle lens camera is presented. The proposed system consists of; i) lens distortion correction using space-varying interpolation kernels and ii) image restoration based on the local self-similarity. The correction process for the geometric distortion produced by a wide-angle lens results in radial distortion artifacts caused by non-linear resampling. To reduce such artifacts, the proposed algorithm uses space-varying interpolation kernels derived from the lens calibration data. The corrected image is further enhanced using self-example-based image restoration. Experimental results demonstrate the proposed method can correctly remove the geometric distortion and further enhance the quality of the radially interpolated image.*[1]

Index Terms — wide-angle lens, distortion correction, image enhancement, local self-similarity

I. Introduction

Recently, a wide-angle lens has become popular for not only photography but also various digital imaging devices such as surveillance systems, vehicle rearview cameras, and endoscopes. Despite many advantages, wide-angle view images acquired by a single camera cannot avoid radial distortion in the peripheral region, which results in significant degradation of the image quality.

To solve this problem, several lens distortion correction methods have been studied in the context of the camera calibration. Devernay *et al.* estimated parameters of the polynomial model for a wide-angle lens [1]. Hughes *et al.* proposed a fisheye lens calibration method by extracting the vanishing point [2]. Park *et al.* proposed a lens distortion correction method using the ideal image coordinates [3]. Lee *et al.* used a planar checkerboard pattern to estimate distortion parameters and the center of distortion [4]. Above mentioned methods rely on the camera calibration which defines the relationship between the undistorted and the correspondingly distorted coordinates. The common problems of these methods are the non-uniform image resolution and gradually increasing aliasing artifact in the radial direction since conventional interpolation methods cannot completely cover the non-uniform distortion. As a result, aliased high frequency components in the central region and blurred details in the peripheral region significantly degrade the image quality and the performance of object recognition.

In this paper, a novel, application-specific lens distortion correction method using space-varying interpolation kernels and the corresponding image enhancement method are presented. The combined algorithm consists of two functional modules including; i) distortion correction using scalable Gaussian interpolation kernels and ii) edge enhancement using self-examples based on the local self-similarity.

The rest of the paper is organized as follows. Image degradation model is presented for the geometric distortion correction of radial distortion and the resulting artifacts in section II. The details of the proposed correction and enhancement methods are presented in section III. Experimental results using the proposed and existing algorithms are given in section IV, and section V concludes the paper.

II. Theoretical Background of Distortion Correction and the Resulting Artifacts

In this section, geometric lens distortion correction methods and the corresponding artifacts are briefly described for the theoretical background of the proposed work.

A. Correction of Geometric Distortion

Theoretically, distortion of a wide-angle lens occurs in a radial manner. In other words, distortion is symmetric to the optical axis that passes through the center of an image. As a result, the amount of distortion depends on the distance from the image center.

A general distortion correction method defines the relationship between distorted and undistorted coordinates, such as

$$x_D = \alpha(r_U) \cdot x_U \,,\; y_D = \alpha(r_U) \cdot y_U \,, \tag{1}$$

[1] This research was supported by Basic Science Research Program through National Research Foundation (NRF) of Korea funded by the Ministry of Education, Science and Technology (2009-0081059) and Samsung Electronics.

Donggyun Kim is with the Department of Image, Chung-Ang University, 156-756, Seoul, Korea (e-mail: deepain83@gmail.com).

Jinho Park is with the Department of Image, Chung-Ang University, 156-756, Seoul, Korea (e-mail: dkskzmffps@gmail.com).

Junghoon Jung is with the System LSI, Samsung Electronics Co., Ltd, 446-811, Yongin, Korea (e-mail: junghoon.jung@samsung.com).

Taechan Kim is with the System LSI, Samsung Electronics Co., Ltd, 446-811, Yongin, Korea (e-mail: taechan@samsung.com).

Joonki Paik is with the Department of Image, Chung-Ang University, 156-756, Seoul, Korea (e-mail: paikj@cau.ac.kr).

Contributed Paper
Manuscript received 12/26/13
Current version published 03/20/14
Electronic version published 03/20/14.

where (x_U, y_U) represents the Cartesian coordinates in the undistorted image plane, (x_D, y_D) the Cartesian coordinate in the distorted image plane, r_U the distance from the center of image $(0,0)$ to (x_U, y_U) in the undistorted image, r_D the distance from the image center $(0,0)$ to (x_D, y_D) in the distorted image, and $\alpha(r_U)$ the function that defines the ratio r_D / r_U. The function can be modeled as either a high-order polynomial or a logarithm. A practical example of α is shown in Fig. 1. If $C = 1$, the distortion is corrected to generate an output whose size is the equal to that of the input image. Each pixel in the distorted image goes to the corresponding position in the undistorted image coordinate, but blank pixels are generated in the corrected image near the center of horizontal and vertical sides. If $B = 1$, the corrected image becomes a cropped rectangle. In section III, the proposed algorithm starts with a given α that is proportional to the standard deviation of Gaussian interpolation kernels.

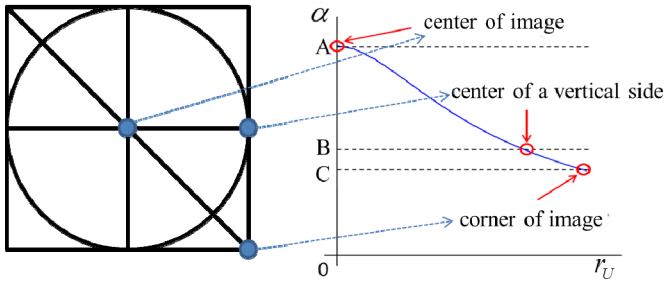

Fig. 1. (a) Coordinate of the undistorted image and (b) an example of the corresponding function $\alpha(r_U)$.

B. Artifacts of Conventional Distortion Correction

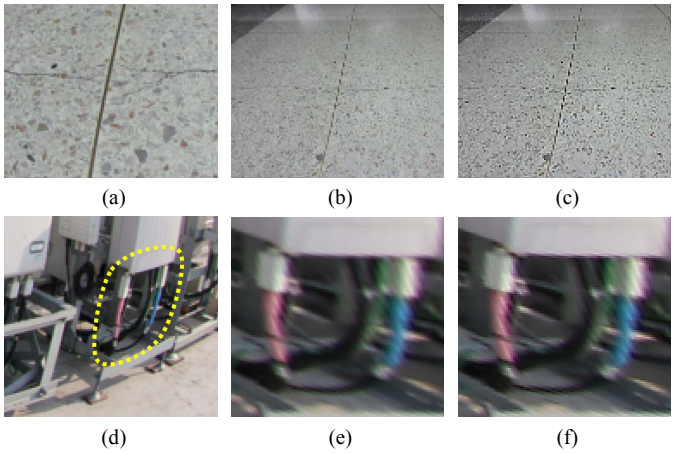

Fig. 2. Two types of artifacts of conventional correction methods for a wide-angle lens camera; (a) the center portion of an input distorted image, (b-c) corrected results with aliasing artifacts using bilinear and higher-order interpolation methods, respectively, (d) the corner portion of the input distorted image, (e-f) corrected results with jagging artifacts using bilinear interpolation and higher-order interpolation methods, respectively.

Radial distortion occurs in a space-variant, non-linear manner. However, conventional correction methods use space-invariant interpolation kernels for inverse mapping. As shown in Fig. 1(b), $\alpha(0) = A$ is usually greater than the unity and the central region of the image suffers the down-sampling effect, which results in aliasing as shown in Figs. 2(b) and 2(c). The aliasing artifacts cannot be easily removed using conventional low pass filter because the sampling rate varies along the radial direction. On the other hand, the up-sampled peripheral region cannot recover the original resolution and contains radially stretched jaggies as shown in Figs. 2(e) and 2(f).

III. Example-based Lens Distortion Correction

In order to remove the artifacts shown in Fig. 2, scalable Gaussian interpolation kernels are employed as a weighted averaging filter, where the standard deviation of a Gaussian filter adaptively changes. For further enhancing the blurred edges, a novel image enhancement method is presented based on the self-similarity of the input image.

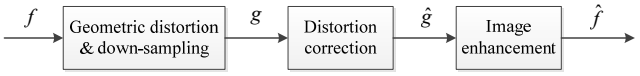

Fig. 3. Basic concept of image degradation model and the proposed distortion correction and image enhancement algorithm.

Fig.3 outlines the image degradation model and the proposed distortion correction and image enhancement algorithm. f represents an ideal distortion-free image, g the input image acquired by a wide-angle lens camera, $\hat{g}$ the distortion corrected image, and $\hat{f}$ the final image. The space-varying Gaussians interpolation kernels and the self-example-based image enhancement are respectively described in the following subsections.

A. Space-Varying Gaussian Interpolation Kernels

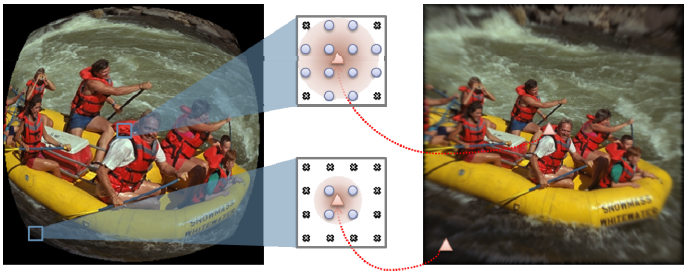

Fig. 4. Concept of space-varying Gaussian interpolation kernels. In the central part of the image, a large interpolation kernel (top) can be used since there is down-sampling. On the other hand, in the corner of the image, a smaller interpolation kernel (bottom) is needed to prevent the blur.

Fig. 4 shows the concept of the scalable Gaussian interpolation kernels. Correction of the distorted image is performed by a geometric transformation that needs to find

intensity values of off-grid pixels using an interpolation kernel such as a weighted averaging filter. As shown in Fig. 4, the size of the proposed Gaussian interpolation kernel decreases as the distance from the image center increases. The intensity value $\hat{g}(x_U, y_U)$ of a pixel in the corrected image is computed as

$$\hat{g}(x_U, y_U) = \sum_{m=-2}^{2} \sum_{n=-2}^{2} G\left(\alpha(r_U), \sqrt{m^2+n^2}\right) \cdot g(x_D + m, y_D + n), \quad (2)$$

where g represents the input image, $g(x_D + m, y_D + n)$ the 5×5 neighbor of $g(x_D, y_D)$, and G the scalable Gaussian interpolation kernel expressed as

$$G\left(\alpha(r_U), \sqrt{m^2+n^2}\right) = \frac{1}{\sqrt{2\pi\sigma^2}} \exp\left\{-\frac{m^2+n^2}{2\sigma^2}\right\}, \quad (3)$$

where σ varies according to $\alpha(r_U)$ in the following manner

$$\sigma = \frac{\alpha(r_U)}{K}, \quad (4)$$

where K is a constant that controls the trade-off between the amount of anti-aliasing and fuzziness of edge. In this work, $K = 2$ was used for the experimentally optimal result.

B. Self-example-based Image Enhancement

Image resampling in the geometric transformation process results in blurring artifacts. More specifically, it is impossible to find the optimal interpolation method that is free from both jagging and blurring artifacts in the corrected image. A practical solution for this problem is to use a space-variant Gaussian interpolation for minimizing jagging artifact, then to use an additional image enhancement algorithm to reduce blurring artifacts. In this subsection, a novel example-based enhancement algorithm is presented based on the local self-similarity.

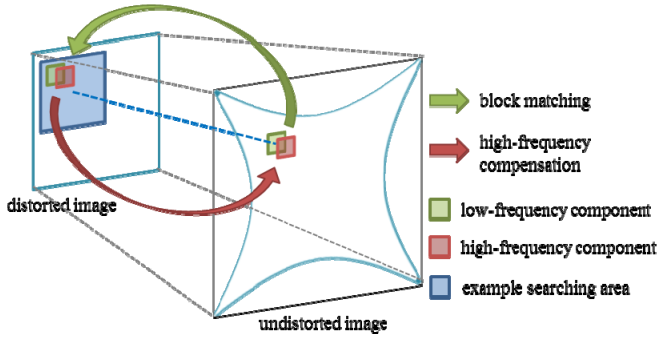

Fig. 5. The proposed enhancement method using LSS

The original concept of the local self-similarity has been proposed by Suetake *et al.* and Freedman *et al.* for image super-resolution [5], [6]. The fundamental assumption of the local self-similarity is that for every patch in the image, similar patches can be found in its downscaled (or smoothed) version in localized regions around the same relative coordinates. This assumption can be extended for enhancing the geometrically corrected image for sufficiently small patches.

The proposed enhancement scheme shares the fundamental assumption of the local self-similarity with the Freedman *et al.*'s original work as shown in Fig. 5 [6]. However the novel contribution of the proposed work is two-fold: i) the patch decomposition process can be simply implemented without using the complex wavelet transform, and ii) the optimal ratio of down- and up-sampling can be determined by the function $\alpha(r_U)$ given in (1). In the central region, $\alpha \geq 1$ and almost no high-frequency component is decomposed from patches since there is no up-sampling. Therefore, it prevents overshooting in central region that has clear edges. On the other hand in the periphery, where $\alpha < 1$, more high-frequency components are decomposed from patches to enhance the blurred edges. Let $\hat{f}(x_U, y_U)$ represent the intensity value of a pixel in the enhanced version of corrected image, then both undistorted patch and corresponding example patches can be respectively expressed as, for $-\frac{B_H}{2} \leq k, l \leq \frac{B_H}{2}$

$$\begin{aligned} \hat{g}^P_{x_U, y_U}(k,l) &= \hat{g}(x_U + k, y_U + l), \\ g^P_{x_D+i, y_D+j}(k,l) &= g(x_D + k + i, y_D + l + j), \end{aligned} \quad (5)$$

where $\hat{g}^P_{x_U, y_U}(k,l)$ represents the undistorted patch centered on (x_U, y_U), $g^P_{x_D+i, y_D+j}(k,l)$ the example patch in the distorted image centered on $(x_D + i, y_D + j)$, $B_H \times B_H$ the patch size, and (i, j) the displacement vector. The optimal displacement vector (i_m, j_m) is estimated by minimizing the sum of absolute difference (SAD) as, for $-5 \leq i, j \leq 5$,

$$(i_m, j_m) = \arg\min_{(i,j)} \sum_k \sum_l \left| \hat{g}^P_{x_U, y_U}(k,l) - g^P_{x_D+i, y_D+j}(k,l) \right|, \quad (6)$$

where $\hat{g}^{LP}$ and g^{LP} respectively represent low pass filtered patches by filtering the $\hat{g}^P$ and g^P with Gaussian filter whose deviation is $1/\alpha(r_U)$. An example patch $g^P_{x_D+i_m, y_D+j_m}$ is then selected to compensate the high-frequency. The high-frequency component is simply calculated by subtracting $g^{LP}_{x_D+i_m, y_D+j_m}$ from $g^P_{x_D+i_m, y_D+j_m}$. $\hat{f}(x_U, y_U)$ is finally calculated as, for all (x_U, y_U) and ,

$$\hat{f}(x_U + k, y_U + l) = \hat{g}(x_U + k, y_U + l) + g^{HP}_{x_D+i_m, y_D+j_m} \cdot \frac{1}{{B_H}^2}, \quad (7)$$

where $g^{HP}_{x_D+i_m, y_D+j_m}$ represents the high-frequency component of the selected example patch with displacement vector (i_m, j_m), and $1/{B_H}^2$ the normalizing term for overlapped patches.

IV. Experimental Results

Both optically simulated and real images are tested for demonstrating the theoretical correctness of the proposed method and the subjective measure of performance.

For the first experiment, an optical simulator was used to generate geometrically distorted images instead of using a real distorted image by a specific lens. Given a distorted input image, bilinear interpolation and the proposed space-variant Gaussian interpolation methods were used to correct the input distorted images. Interpolation methods used in this work are different from conventional rectangular grid-based methods since the geometric correction requires interpolation in the radial direction. For this reason, there are not many interpolation algorithms except the bilinear method to the best of authors' knowledge. The corrected images were further enhanced by the proposed local self-example-based image restoration method.

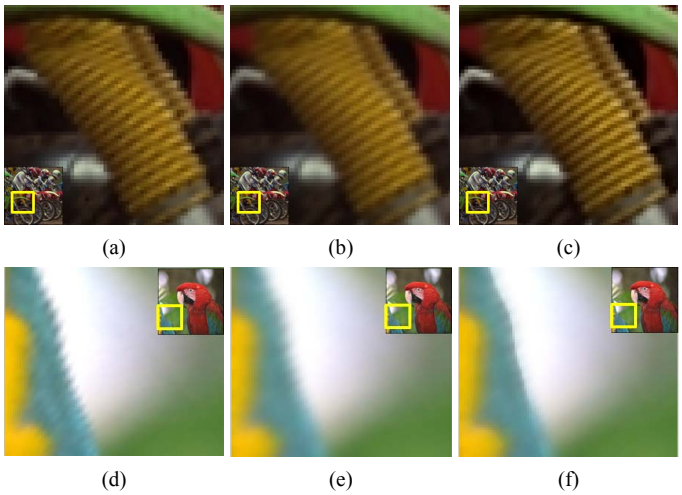

Fig. 6. Correcting an optically simulated distortion (top: central region, bottom: peripheral region) using conventional and proposed methods. (a, d) bilinear interpolation, (b, e) the proposed space-variant Gaussian interpolation, and (c, f) the proposed self-example-based enhancement method

Fig. 6 compares the performance of three different correction methods. The top row shows the central region of the image to evaluate the performance of aliasing removal. Fig. 6(a) shows the result of bilinear interpolation, where a significant amount of aliasing is observed in the wrinkles of the shock absorber. Fig. 6(b) shows the result of the proposed radial distance-adaptive Gaussian interpolation method. Most of aliasing is successfully smoothed out. Fig. 6(c) shows the result of the proposed self-example-based enhancement method. Most of blurry edges are sharpened without overshooting. The bottom row of Fig. 6 shows the peripheral region of the image to evaluate the performance of restoring blurred details. In Fig. 6(d), a significant amount of blur and stretched jaggies are observed. Fig. 6(e) shows that most of jaggies are well smoothed. Fig. 6(f) shows that most of blurry edges are sharpened without overshooting.

For objective comparison, peak-to-peak signal-to-noise ratio (PSNR), structural similarity measure (SSIM) [7], and the modulation transfer function (MTF) values are calculated for evaluating the restoration performance of preserving the high-frequency details. The MTF is calculated by measuring slant of manually selected edges which can have maximum value 1 Cycle/Pixel. The overshooting ratio is also calculated for analyzing the performance of minimizing restoration artifacts such as ringing artifact. It is calculated by measuring the ratio between peak to peak of manually selected edges and stabled dynamic range of the edge.

TABLE I
QUANTITATIVE ASSESSMENT (30 RESULTS AVERAGED)

	Bilinear	Proposed Gaussian	Proposed Enhancement
PSNR	**29.0739**	27.4516	28.5769
SSIM	**0.9096**	0.8558	0.8772
MTF50 (Cy/Pxl)	0.16	0.107	**0.18**
Overshooting (%)	11.2	8.26	**10**

Table. I shows PSNR and SSIM values evaluated on the entire images, and the result of analyzing edges on periphery using the MTF and overshooting values. Although the bilinear methods give higher PSNR and SSIM values than the proposed method, aliasing artifacts and jagged edges are not acceptable as shown in Figs. 6(a) and 6(d), respectively. On the other hand, the propose method including the self-example-based enhancement provides acceptable results, and higher MTF and lower Overshooting values demonstrates the performance of preserving details and minimizing restoration artifacts.

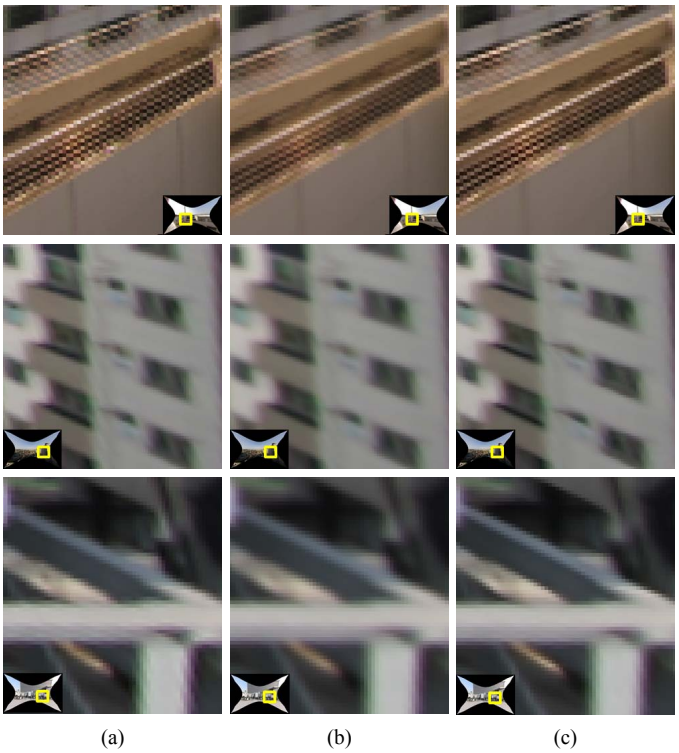

Fig. 7. Correcting a real lens distortion (top: central region, middle and bottom: peripheral regions) using conventional and proposed methods. (a) bilinear interpolation, (b) the proposed space-variant Gaussian interpolation, and (c) the proposed self-example-based enhancement method.

Fig. 7 compares the performance of three different correction methods using real images. Figs. 7(a) show the result of bilinear interpolation, where a significant amount of aliasing and jagging artifacts are observed. Figs. 7(b) show the result of the proposed radial distance-adaptive Gaussian interpolation method. Most of artifacts are successfully smoothed out. Figs. 7(c) show the result of the proposed self-example-based enhancement method. Most of blurry edges are sharpened without overshooting.

V. Conclusion

A novel geometric correction and enhancement method is proposed for high quality images acquired by a wide-angle lens camera. A scalable Gaussian interpolation kernel is proposed for removing aliasing in the central region of the image and stretched jaggies in the periphery. Because the size of an interpolation kernel decreases according to calibration data, aliasing and stretched jaggies are successfully removed without losing the sharpness. For further enhancing the geometrically corrected image, the self-example-based enhancement method is proposed to restore blurred edges in the periphery of the image. As shown in experimental results, the proposed algorithm enhances the distorted image without aliasing, stretched jaggies or edge overshooting. The proposed method can be used in various applications with a wide-angle lens camera such as consumer surveillance systems, vehicle rearview cameras, and endoscopes.

References

[1] F. Devernay, and O. Faugeras, "Straight lines have to be straight," *Machine Vision and Applications*, vol. 13, no. 1, pp.14-16, Aug. 2001.

[2] C. Hughes, R. McFeely, P. Denny, M. Glavin, and E. Jones, "Equidistant fish-eye perspective with application in distortion centre estimation," *Image and Vision Computing*, vol. 28, no. 3, pp. 538-551, Mar. 2010.

[3] J. Park, S. Byun, and B. Lee, "Lens distortion correction using ideal image coordinates," *IEEE Trans. Consumer Electron.,* vol. 55, no. 3, pp. 987–991, Aug. 2009.

[4] S. Lee, S. Lee, and J. Choi, "Correction of radial distortion using a planar checkerboard pattern and its image," *IEEE Trans. Consumer Electron.*, vol. 55, no. 1, pp. 27-33, Feb. 2009.

[5] N. Suetake, M. Sakano, and E. Uchino, "Image super-resolution based on local self-similarity," *Optical Review*, vol. 15, no. 1, pp. 26-30, Jan. 2008.

[6] G. Freedman and R. Fattal, "Image and video upscaling from local self-examples," *ACM Trans. Graphics*, vol. 30, no. 2, pp. 12, Apr. 2011.

[7] Z. Wang, A. Bovik, H. Sheikh, and E. Simoncelli, "Image quality assessment: From error visibility to structural similarity," *IEEE Trans. Image Processing*, vol. 13, no, 4, pp. 600-612, Apr. 2004.

BIOGRAPHIES

Donggyun Kim (S'11) was born in Busan, Korea in 1983. He received B.S. and M.S. degrees in electronic and electrical engineering from Chung-Ang University, Korea, in 2007 and 2009, respectively. Currently, he is pursuing the Ph.D. degree in image processing at Chung-Ang University. His research interests include image restoration, digital auto-focusing, lens distortion correction, and image super-resolution.

Jinho Park (S'13) was born in Seoul, Korea in 1987. He received the B.S. degree in electronic engineering from Suwon University, Korea, in 2013. Currently, he is pursuing the M.S. degree in image processing at Chung-Ang University. His research interests include image enhancement, super-resolution, and real-time object tracking

Junghoon Jung received BS, MS and Ph.D degrees in electronics engineering from Chung-Ang University, Seoul, Korea, in 1997, 1999 and 2004, respectively. He joined Humax Corporation in 2004, and developed image enhancement algorithms for digital television. From 2007, he is in charge of developing image signal processors for mobile camera in Samsung Electronics. His research interests include camera image signal processor, image enhancement, extended depth-of-field and computational photography.

Taechan Kim (SM'12) has over 25 years experiences working on digital TV, SoC design, micro-controller and CCD/CMOS image sensor in Samsung Electronics, and currently is a technical vice-president in Samsung Electronics focusing on development of CMOS image sensor and image signal processor. His research interests include camera SoC design, image signal processor, image enhancement and computational photography. He is a senior member of IEEE, and an executive member in Institute of Electronics Engineers of Korea (IEEK). He received Ph.D degree in Electronics engineering from Korea University, Seoul, Korea, in 2004.

Joonki Paik (M'89 –SM'12) was born in Seoul, Korea in 1960. He received the B.S. degree in control and instrumentation engineering from Seoul National University in 1984. He received the M.S. and the Ph.D. degrees in electrical engineering and computer science from Northwestern University in 1987 and 1990, respectively. From 1990 to 1993, he joined Samsung Electronics, where he designed the image stabilization chip sets for consumer's camcorders. Since 1993, he has joined the faculty at Chung-Ang University, Seoul, Korea, where he is currently a Professor in the Graduate school of Advanced Imaging Science, Multimedia and Film. From 1999 to 2002, he was a visiting Professor at the Department of Electrical and Computer Engineering at the University of Tennessee, Knoxville. Dr. Paik was a recipient of Chester-Sall Award from IEEE Consumer Electronics Society, Academic Award from the Institute of Electronic Engineers of Korea, and Best Research Professor Award from Chung-Ang University. He has served the Consumer Electronics Society of IEEE as a member of the Editorial Board. Since 2005, he has been the head of National Research Laboratory in the field of image processing and intelligent systems. In 2008, he has worked as a full-time technical consultant for the System LSI Division in Samsung Electronics, where he developed various computational photographic techniques including an extended depth of field (EDoF) system. From 2005 to 2007 he served as Dean of the Graduate School of Advanced Imaging Science, Multimedia, and Film. From 2005 to 2007 he has been Director of Seoul Future Contents Convergence (SFCC) Cluster established by Seoul Research and Business Development (R&BD) Program. Dr. Paik is currently serving as a member of Presidential Advisory Board for Scientific/Technical policy of Korean Government and a technical consultant of Korean Supreme Prosecutor's Office for computational forensics.